Title	Cerebral hemodynamics synchronized with electroencephalography rhythms during sleep transitions
Sub Title	
Author	内田 (太田), 真理子(Uchida Ota, Mariko)
Publisher	Centre for Advanced Research on Logic and Sensibility The Global Centers of Excellence Program, Keio University
Publication year	2010
Jtitle	CARLS series of advanced study of logic and sensibility Vol.3, (2009.) ,p.159- 164
Abstract	
Notes	Part 2 : Genetics and Development
Genre	Research Paper
URL	http://koara.lib.keio.ac.jp/xoonips/modules/xoonips/detail.php?koara_id=KO12002001-20100331-0159

19 Cerebral Hemodynamics Synchronized with Electroencephalography Rhythms during Sleep Transitions

Mariko Uchida-Ota

Centre for Advanced Research on Logic and Sensibility (CARLS), Keio University

I. Introduction

The brain activity during sleep has been previously observed through the electroencephalography (EEG). It has been recently reported that the changes in the cerebral hemoglobin concentration (Δ[Hb]) measured by the near infrared spectroscopy (NIRS) are synchronized with EEG changes. Hoshi et al. (1994) and Spielman et al. (2000) reported Δ[Hb] were observed in the transitional phase where the alpha rhythm activity in EEG decreased or increased. On the other hand, Kotajima et al. (2005) reported that the increased blood flow in the middle cerebral artery is associated with a decrease in mean arterial blood pressure during the transition from alpha rhythm dominance to theta rhythm dominance. It remains unclear whether Δ[Hb] during sleep synchronized with EEG changes represents the spontaneous brain activity or the systemic circulation activity like the blood pressure.

In this report, we introduce one of our studies using the partial correlation analysis for the detection of Δ[Hb] which is intrinsically synchronized with EEG changes and not affected the blood pressure (Uchida-Ota, et al., 2008).

II. Methods

1. Participants and Measurement

Twelve subjects between 24 and 43 years old (four females and eight males, mean age 33.5 years) participated in this experiment. None had cardiovascular, respiratory, sleep, or nervous disorders. Written informed consent was obtained from each participant before the experiment.

In each participant, we recorded the EEG, the cerebral oxy-hemoglobin and deoxy-hemoglobin concentration changes (Δ[oxy-Hb] and Δ[deoxy-Hb]), the mean arterial blood pressure (MAP), electrooculograms (EOG), and a chin electromyogram (EMG) for 45 to 60 minutes between 14:00 and 16:00. The participants were instructed before the measurement to sleep whenever they became sleepy or wanted to sleep.

The EEG, EOG, and EMG were measured by an EEG system (EEG-1000, Nihon Kohden, Tokyo, Japan). The EEG signals were recorded via Ag-AgCl electrodes at four scalp sites (C3, C4, O1, and O2 according to the International 10-20 system of electrode placement). All the EEG electrodes were linked to the earlobe electrode as a reference of A1 or A2. The signals were sampled at 200 Hz. The Δ[oxy-Hb] and Δ[deoxy-Hb] were measured by an optical topography system (ETG-7000, Hitachi Medical Corporation, Chiba, Japan; sampling rate 10 Hz) at 88 locations by using four 22-probe holders. The MAP (mmHg) was monitored by using an infrared photo-plethysmograph (Finometer, Finapress Medical Systems BV, Arnhem, Netherlands; sampling rate 200 Hz) to measure changes in arterial diameter in the middle knuckle of the left middle finger.

2. Analysis

Sleep stages were scored—according to the EEG, EOG, and EMG signals—at 30-s intervals with polysomnography analysis software (Polysmith QP-260A, Neurotronics, Florida, USA). The sleep states were subdivided into five categories: ‘waking’, ‘REM’, ‘drowsy state’, ‘light sleep’, and ‘deep sleep’. We focused on EEG alpha rhythm and sigma rhythm (sleep spindle) because ‘drowsy state’ and ‘light sleep’ occurred more frequently than other states in the measurements and these rhythms are often observed in these states.

In the signal preprocessing, each EEG, Δ[oxy-Hb], Δ[deoxy-Hb], and MAP signal was transformed appropriately so that the one could be compared with another. EEG signals were processed, at 0.1-s intervals, with a fast Fourier transform with a temporal Hann window of 512 data points. The resultant time-dependent

spectrum was transformed into the alpha-range-averaged power values (EEGFα; the alpha rhythm range is 7.5–11.5 Hz) or the sigma-range-averaged power values (EEGFσ; the sigma rhythm range is 12.0–16.0 Hz). The temporal sequence of EEGFα or EEGFσ was denoted x_{EEGF}. The Δ[oxy-Hb], Δ[deoxy-Hb] and MAP signals were transformed with a filter having a pass band from 0.05 to 0.35 Hz and were denoted x_{Hb} and x_{MAP}. These temporal sequences of x_{EEGF}, x_{MAP}, and x_{Hb} were clipped at 120-s lengths. Each clipped data which did not contain noise due to body or eye movement was normalized and evaluated to find out whether the Δ[Hb] was free from MAP influence and intrinsically correlated with the EEGF by the following partial correlation analysis.

We calculated the partial correlation coefficient $\rho_{\mathrm{EH\cdot P}}$ given by

$$\rho_{\mathrm{EH\cdot P}} = \frac{\rho_{\mathrm{EH}} - \rho_{\mathrm{PH}}\rho_{\mathrm{EP}}}{\sqrt{1-\rho_{\mathrm{PH}}^2}\sqrt{1-\rho_{\mathrm{EP}}^2}}, \tag{1}$$

where

$$\rho_{\mathrm{EH}} = \int_l^m x_{\mathrm{EEGF}}(t)\ \ x_{\mathrm{Hb}}(t + T_{\mathrm{EEGF,Hb}})dt, \tag{2}$$

$$\rho_{\mathrm{PH}} = \int_l^m x_{\mathrm{MAP}}(t)\ \ x_{\mathrm{Hb}}(t + T_{\mathrm{MAP,Hb}})dt, \tag{3}$$

and

$$\rho_{\mathrm{EP}} = \int_l^m x_{\mathrm{EEGF}}(t)\ \ x_{\mathrm{MAP}}(t + T_{\mathrm{EEGF,Hb}} - T_{\mathrm{MAP,Hb}})dt. \tag{4}$$

$T_{\mathrm{EEGF,Hb}}$ and $T_{\mathrm{MAP,Hb}}$ are time lags providing the maximum absolute cross-correlation. The integration interval m-l was set at 120-$|T|$ s. We respectively set ρ_{EH}, ρ_{PH}, and ρ_{EP} to the coefficients of the maximum cross-correlations between EEGF and Δ[Hb] given by Eq. (2), between MAP and Δ[Hb] given by Eq (3), and between EEGF and MAP given by Eq. (4). The clipped data satisfying $|\rho_{\mathrm{EH\cdot P}}| > 0.7$ were extracted as the intrinsic synchronization data between EEGF and Δ[Hb].

We estimated the most likely anatomical locations of all Δ[Hb] measurement positions using the software for the registration of Δ[Hb] data to the standard Montreal Neurological Institute (MNI) brain template (Okamoto et al., 2004).

III. Results

For a reference, Figure 1(a) and (b) show a typical clipped data satisfying criteria for the detection of the intrinsic synchronization (ISync) between EEGF and Δ[Hb] ($|\rho_{\mathrm{EH\cdot P}}| > 0.7$). In ISync between EEGF$\alpha$ and Δ[Hb], Δ[oxy-Hb] and Δ[deoxy-Hb]

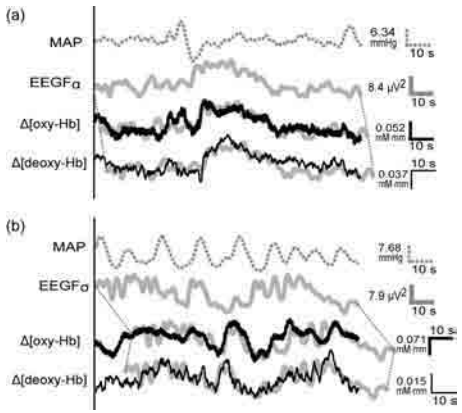

Figure 1. Time course examples for MAP, EEGF, Δ[oxyHb], and Δ[deoxyHb]. (a) In an example of the intrinsic synchronization between EEGFα and Δ[Hb], Δ[oxyHb] followed EEGFα at a time lag of 1.2 s and Δ[deoxyHb] followed EEGFα at a time lag of 2.3 s. (b) In an example of the intrinsic synchronization between EEGFσ and Δ[Hb], Δ[oxyHb] followed EEGFσ at a time lag of 15.8 s and Δ[deoxyHb] followed EEGFσ at a time lag of 12.5 s.

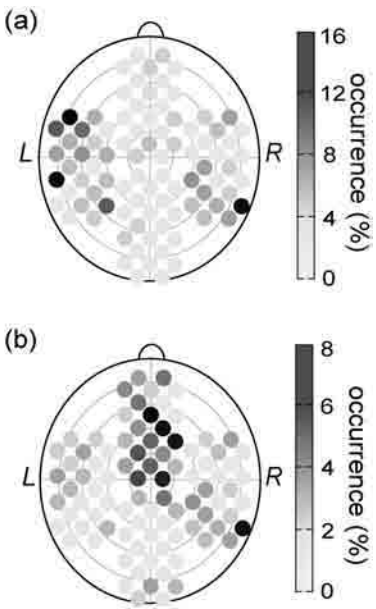

Figure 2. (a) Spatial distributions of the intrinsic synchronization between EEGFα and Δ[Hb]. (b) Spatial distributions of the intrinsic synchronization between EEGFσ and Δ[Hb]. The gray value at each position indicates the mean occurrence ratio over all subjects.

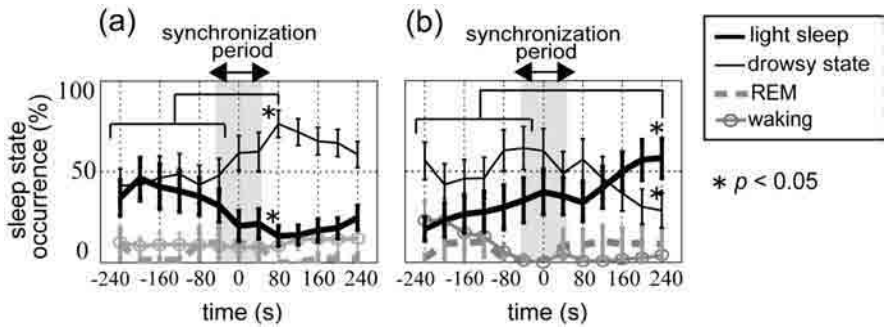

Figure 3. Transition of the occurrence probability for sleep states in vicinity of the period when intrinsic synchronization appeared. The gray zones including time 0 indicate the period in which the intrinsic synchronization appeared. Friedman's ANOVA with *post hoc* multiple comparisons was executed with p <0.05, and each occurrence probability after time 0 was compared with the mean of occurrence probabilities prior to 0. (a) Synchronization between EEGFα and Δ[Hb] was observed in the transition where the occurrence probability of light sleep decreased. (b) Synchronization between EEGFσ and Δ[Hb] was observed in the transition where the occurrence probability of light sleep increased.

are respectively positively and negatively correlated with EEGFα (Figure 1(a)). In ISync between EEGFσ and Δ[Hb], Δ[oxy-Hb] and Δ[deoxy-Hb] are respectively negatively and positively correlated with EEGFσ (Figure 1(b)). These correlation polarities and the values of time lag of Δ[oxy-Hb] and Δ[deoxy-Hb] behind EEGF ($T_{\mathrm{EEGF,Hb}}$) were consistent with other clipped data satisfying the criteria.

We examined the spatial distributions where the ISync occurred. The ISync between Δ[Hb] and EEGFα appeared more frequently in the left inferior frontal gyrus and the right middle temporal gyrus (Figure 2(a)) and ISync between Δ[Hb] and EEGFσ appeared more frequently in the right medial part of superior frontal, middle frontal, and angular gyri (Figure 2(b)). We also examined the sleep states in the vicinity of the period when ISync phenomena occurred. The ISync between Δ[Hb] and EEGFα were observed in the transition from 'light sleep' to 'drowsy state' (Figure 3(a)). The ISync between Δ[Hb] and EEGFσ were observed in the transition from 'drowsy state' to 'light sleep' (Figure 3(b)).

IV. Discussion

By detecting the intrinsic synchronization between EEG activity and cerebral hemodynamics, we revealed the typical features of change in cerebral hemoglobin

concentrations as the spontaneous brain activity rather than the propagation of blood pressure in the specific sleep transitions. These features are consistent with previous studies using the functional magnetic resonance imaging (fMRI). For example, fMRI response to alpha rhythm activity appeared in the prefrontal and temporal gyri (Laufs et al., 2003), and fMRI response to sigma rhythm activity appeared in superior frontal gyrus (Shaubus et al., 2007). The inferior, superior and middle frontal gyri are known to be connected with the mediodorsal and laterodorsal thalamic nuclei driving the sigma rhythm (Fuster, 1997). The middle temporal and angular gyri have the functional connectivity with the hypothalamic region (Kaufmann et al., 2006). Therefore, the intrinsic synchronization between EEGF and Δ[Hb] in this study may reflect the thalamocortical interaction and the connectivity between the hypothalamus and the cortex.

Acknowledgement

This study was supported by the Core Research for Evolutional Science and Technology (CREST) project of the Japan Science and Technology Agency. The author thanks Dr. N. Tanaka, Dr. A. Maki, and Dr. H. Sato for technical supports and useful remarks.

References

Hoshi Y, Mizukami S, Tamura M, 1994 Dynamic features of hemodynamic and metabolic changes in the human brain during all-night sleep as revealed by near-infrared spectroscopy. *Brain Research*, **652**: 257–262.

Kotajima F, Meadows GE, Morrell MJ, and Corfield DR, 2005 Cerebral blood flow changes associated with fluctuations in alpha and theta rhythm during sleep onset in humans. *Journal of Physiology*, **568(1)**: 305–313.

Laufs H, Krakow K, Sterzer P, Eger E, Beyerle A, Salek-Haddadi A, Kleinschmidt A, 2003 Electroencephalographic signatures of attentional and cognitive default modes in spontaneous brain activity fluctuations at rest. *PNAS*, **100(19)**; 11053–11058.

Okamoto M, Dan H, Sakamoto K, Takeo K, Shimizu K, Kohno S, Oda I, Isobe S, Suzuki T, Kohyama K, Dan I, 2004 Three-dimensional probabilistic anatomical cranio-cerebral correlation via the international 10–20 system oriented for transcranial functional brain mapping. *NeuroImage*, **21**: 99–111.

Schabus M, Dang-Vu TT, Albouy G, Balteau E, Boly M, Carrier J, Darsaud A, Degueldre C, Desseilles M, Gais S, Phillips C, Rauchs G, Schnakers C, Sterpenich V, Vandewalle G, Luxen A, Maquet P, 2007 Hemodynamic cerebral correlates of sleep spindles during human non-rapid eye movement sleep. *PNAS*, **104(32)**; 13164–13169.

Spielman AJ, Zhang G, Yang C, D'Ambrosio P, Serizawa S, Nagata M, von Gizycki H, and Alfano RR, 2000 Intracerebral hemodynamics probed by near infrared spectroscopy in the transition between wakefulness and sleep. *Brain Research*, **866**: 313–325.

Uchida-Ota M, Tanaka N, Sato H, Maki A, 2008 Intrinsic correlations of electroencephalography rhythms with cerebral hemodynamics during sleep transitions. *NeuroImage*, **42**: 357–368.